Experimental investigation on streamer inception from artificial hydrometeors

PAPER • OPEN ACCESS

Experimental investigation on streamer inception from artificial hydrometeors

To cite this article: S Mirpour and S Nijdam 2022 *Plasma Sources Sci. Technol.* **31** 105009

OPEN ACCESS
IOP Publishing

Plasma Sources Science and Technology

Plasma Sources Sci. Technol. **31** (2022) 105009 (9pp)

https://doi.org/10.1088/1361-6595/ac95be

Experimental investigation on streamer inception from artificial hydrometeors

S Mirpour* **and S Nijdam**

Department of Applied Physics, Eindhoven University of Technology, PO Box 513, 5600 MB Eindhoven, The Netherlands

E-mail: s.mirpour@tue.nl

Received 12 May 2022, revised 20 August 2022
Accepted for publication 28 September 2022
Published 20 October 2022

Abstract

In this study we use an experimental investigation to shed light on the lightning inception problem. From atmospheric observations, it is known that the electric fields in thunderclouds are significantly lower than required for electric breakdown in air. One theory to explain lightning inception is that hydrometeors, i.e. any liquid or solid water particles formed in the atmosphere, greatly enhance the local electric field and can thereby initiate an electron avalanche leading to a streamer discharge. In this study, we investigate streamer initiation in the presence of artificial particles with different shapes. A metal or dielectric (TiO_2) particle is suspended between a high-voltage and a grounded planar electrode which are separated by 16 cm in 50 mbar air. The particles are shaped as ellipsoids with a length of 8, 4, 2, and 1 cm and with different aspect ratios. A negative high voltage pulse is applied with a rise time of 30 ns, a pulse width of 1–10 μs, a repetition rate of 1 Hz, and a maximum voltage between 1 and 50 kV. Results show that the required background electric field for breakdown in the presence of a dielectric particle is decreased to 0.4 times the air breakdown field. Moreover, we observed bipolar streamer development from the particles where negative streamers are thicker and slightly slower than positive streamers. Finally, we found that streamers from longer particles are thicker and faster.

Keywords: streamer inception, hydrometeors, lightning

(Some figures may appear in colour only in the online journal)

1. Introduction

One of the unanswered fundamental questions in atmospheric electricity physics is the lightning inception issue [1–4]. Observations have shown that the electric field of a thundercloud is much lower (approximately 1/10) than the critical electric field, E_k, required for discharge initiation [5]. One of the main theories to explain this is a streamer-based mechanism for lightning initiation [6]. In this model, a system consisting of a few successful positive streamers can lead to a significant electric-field enhancement at their origin. However, in this model, a main question that remains unanswered is how the very first streamer is initiated under a sub-breakdown field. One main hypothesis that has been developed and discussed is lightning inception by hydrometeors, in which electric fields can be significantly enhanced near the extremities. A more advanced model that has been recently suggested by [7] states that the lightning initiation process begins with an 'initiating event' such as a narrow bipolar event which changes the non-conducting air into a conducting environment. This initiating event would then be followed by positive streamer development flashes which are able to merge together and form plasma formation chains or small networks. This process ultimately would lead to a bidirectional leader. Finally, the breakdown stage is started where bidirectional leaders merge together. The lightning flash would then transition to the negative stepped leader phase after a series of such events.

* Author to whom any correspondence should be addressed.

A streamer is initiated when an electron is available in a relatively high electric field near the hydrometeor tip where the ionization coefficient is approximately higher than the attachment coefficient. Under such conditions, the number of electrons can start to increase exponentially and eventually result in an electron avalanche. The number of produced electrons should be higher than the so-called Meek criteria [8], which has recently been revisited by Montijn and Eber [9]. As soon as the number of electrons meets the Meek criterion, the space charge is sufficient to initiate a streamer. It is also worth mentioning that this criteria is still under discussion since it describes discharge initiation by single electron avalanches while experimental investigations have shown the multi-avalanche nature of streamer formation. In this case, the large number of primary electrons leads to the formation of streamers at significantly lower voltages [10].

Streamer inception from hydrometeors has been the focus of quite a few theoretical and experimental studies. In most of these, the hydrometeor or ice crystal is considered as a suspended electrode in the gap and is not connected to an external circuit. Petersen *et al* [11] experimentally investigated streamer inception from ice crystals. They were able to produce ice crystals and place them between two electrodes at low temperatures. They established an empirical formula between the positive corona inception and the temperature and length of the ice particles. They found that positive streamers can be initiated in a lower electric field at temperatures well below -18 °C by longer ice crystals. Furthermore, they showed that in addition to ice crystal length, tip sharpness can play an important role. Although ice crystals with sharper tips can increase the field enhancement, an ice crystal with a very sharp tip (<100 μm) can also inhibit positive streamers. In another experiment, Mazur *et al* [12] used an array of conducting spherical particles in a large-gap, high-voltage setup. They observed bidirectional and bipolar leader development from the particles. They showed that the size of the particle can influence the duration of the discharge. Some questions were not answered in their study, such as the streamer inception point and propagation velocity, since their observations were limited by leader development and no investigation was conducted regarding primary streamers development.

On the theoretical and numerical side, there have been more complicated and advanced studies on this topic. Sadighi *et al* [13] modeled a column-shaped ionized patch under sub-breakdown conditions. They found that at an altitude of 7 km, streamers can be initiated from the hydrometeor at $0.3E_k$. This can be achieved for hydrometeors with a length between 5 and 8 mm and an ambient background density on the order of 10^{15} m^{-3}. Because of the importance of the hydrometeor geometry, Dubinova *et al* [14] investigated the requirements for a large ellipsoid hydrometeor as a function of the background field. They found that streamers can be initiated at lower electric fields from longer and sharper particles. More specifically, at an ambient background density of 100 free electrons per cm^3, streamer inception is observable from a hydrometeor with a length of 6 cm and a tip radius-to-length ratio of 0.005 at approximately $0.15E_k$. In addition to the shape and size, a unique feature of ice is its dielectric function, which yields a high dielectric constant (approximately 93) at low frequencies and a low dielectric constant of 3 at high frequencies. This can manifest itself in streamer inception where the very first electrons experience almost a DC field, while streamer propagation occurs on the order of a few ns (MHz to GHz). Dubinova *et al* [15] demonstrated the influence of dielectric properties on streamer propagation and showed that streamers from particles with a dielectric function of ice are lower than those of particles with a constant dielectric permittivity of 93. Notably, when discussing dielectric particles, it is important to consider surface charge accumulation (initial net charge), which was not considered in Dubinova's work. It has been shown that negative charges are accumulated on particles and increase during streamer propagation [16, 17]. This can generally influence the near-tip electric field enhancement, streamer propagation, and inception, especially if we work under repetitive discharges. One important missing piece in theoretical studies is a comparison with experimental data, which can likely show the mentioned effects in a real-life experiment. In our previous work [18], we present a theoretical model which investigates the discharge inception criterion near ellipsoidal hydrometeors. We showed that longer and sharper hydrometeors can enhance the electric field near the hydrometeor tip up to $37E_k$. Furthermore, in line with [15] we found an optimal ellipsoidal aspect ratio of 0.1 for corona inception for representative conditions.

In this study, we implemented an experimental approach to understand the discharge behavior near ice-like dielectric particles and compared that with metal particles. Of primary interest in this work are the effects of particle size and shape on streamer inception near particles. Of secondary importance are streamer propagation properties (velocity and thickness) from different particles to understand the role of particle size and shape and its dielectric profile.

2. Materials and methods

2.1. Experimental conditions

All experiments in this study were performed in a plane-to-plane geometry in which an ellipsoid dielectric or metal particle (a = semi-major and b = semi-minor axis) was suspended by a thin fishing line (diameter of 0.3 mm) between high-voltage and grounded electrodes (see figures 1 and 2). Note that no corona formation was detected from the fishing line. The dielectric and metal ellipsoid particles are composed of titanium dioxide (TiO_2) and brass respectively and have varying different tip radii ($R = b^2/a$) and lengths ($L = 2 \times a$). The dielectric particles were formed by annealing and pressing followed by polishing. Table 1 shows the metal and dielectric particles used for the experiments based on their shape (R/L) and aspect ratio ($AR = b/a$).

In each experiment, a particle was suspended between negative high-voltage and grounded plane electrodes of 20 cm diameter separated by a fixed 15 cm gap distance. The grounded electrode is placed on a fixed larger size grounded electrode fixed to the vacuum vessel. A high-voltage pulse was applied by a circuit consisting of a high-voltage semiconductor

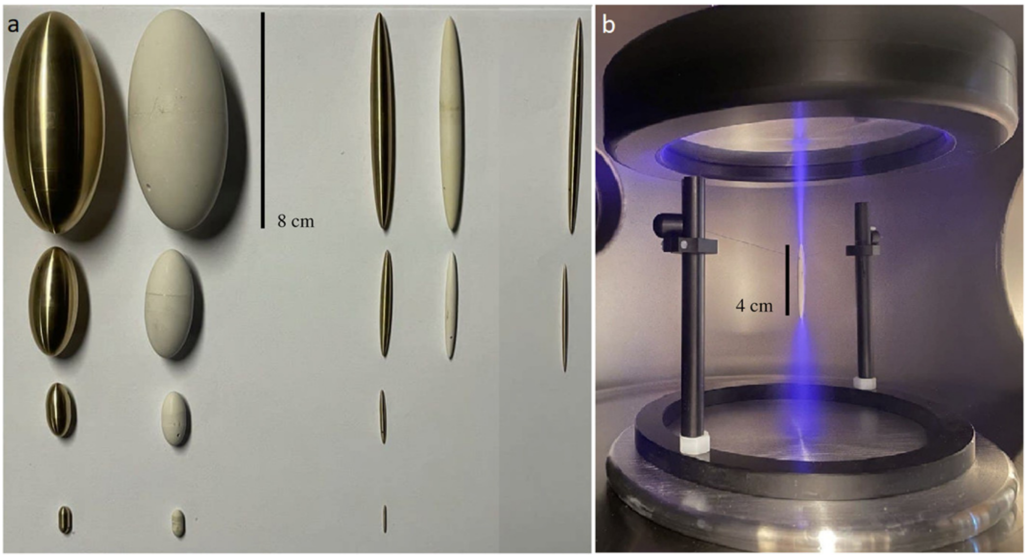

Figure 1. (a) Metal (brass) and dielectric (TiO_2) particles used for this experiment, (b) long exposure camera image of discharges with a dielectric particle ($L = 4$ cm and $AR = 0.1$) placed between a negative high-voltage electrode ($V_{HV} = 15$ kV) and a grounded electrode.

switch (HTS 401-10-GSM, Behlke) and a 1 nF high voltage capacitor. This produced a negative high-voltage pulse with a rise time of 40 ns, a repetition rate of 1 Hz, a pulse width of 1–10 ms and a maximum voltage of 60 kV. The experiments were conducted in synthetic air with a composition of 80% N_2 and 20% O_2 at pressure 50 mbar. To prevent discharges between the high-voltage electrode and the vessel body, we used a PVC rounded insulator around the electrode.

2.2. Dielectric properties of TiO_2

To measure the dielectric profile of the dielectric particles, a cylindrical disk from TiO_2 material with a diameter of 3 cm and height of 1 cm was prepared. We measured the permittivity of this material using dielectric material measurement fixtures (1 kHz–5 MHz: Agilent 16451B and 5 MHz–10 GHz: Agilent 16453A) and a network analyzer (E5071C Agilent). Figure 3 shows the measured relative permittivity of TiO_2 and ice (taken from Mavrovic *et al* [19]) as a function of frequency. Below 10^4 Hz, the relative permittivity of ice is approximately 90. In this range, the TiO_2 dielectric constant was measured to be 140 ± 30. The relative permittivity of ice decreases from 90 to 3 at approximately 10 kHz. For TiO_2, the dielectric constant continuously decreases to less than 10. Note that the step in the dielectric constant profile of TiO_2 at 5×10^6 Hz is due to a switch in measurement device at this frequency and has no physical meaning.

2.3. Inception voltage measurements

To collect the photons from the inception phase, a photomultiplier tube (PMT, Hamamatsu H10720-1 10) with 15 cm lens were placed in front of the vessel to capture photons produced by the corona around the particle tips. The PMT output signal showed a peak for each streamer discharge event. When the peak was 3 times higher than the background level, it was recorded as a streamer initiation. Moreover, the PMT signal matches with the current probe signal on the high voltage side. This confirms that the PMT signals are indeed associated with discharge events. The inception voltage is the voltage at which the discharge initiated. The HV pulse width for these measurements was set to $t_{HV} = 10\ \mu$s to give enough time to initiate the discharge.

2.4. Streamers thickness and velocity measurement

To measure the streamer thickness, we used an intensified CCD camera (ICCD, Stanford Computer Optics 4QuickE) with a Nikkor UV 105 mm $f/4.5$ camera lens mounted directly on the camera. The intensifier enabled us to take streamer images with a nanosecond exposure time. The camera was placed in front of the vessel. For better clarity, the output images are rendered in false color. To measure the streamer thickness, the camera gate was open for 300 ns from the beginning of the HV pulse. V_{HV} and t_{HV} of the HV pulse were fixed to 15 kV and 1 μs at 50 mbar, respectively. This is sufficient time for streamers to fully develop and cross the gap. We scaled the applied voltage for different pressures by keeping V/p constant. From the measured images, several cross sections at 0 (tip), 20%, 40%, 60%, 80% and 100% (electrodes) of the gap for upward and downward streamers were obtained. The streamer thickness was measured as the full width at half maximum in that cross section as we did that in the previous studies [20].

To measure the streamer propagation velocity, we obtained two images with a very short camera exposure time (5 ns) when streamers crossed half of the gap. The two images were taken with a difference in exposure delay of 10 ns. The velocity was determined by dividing the distance between streamer head

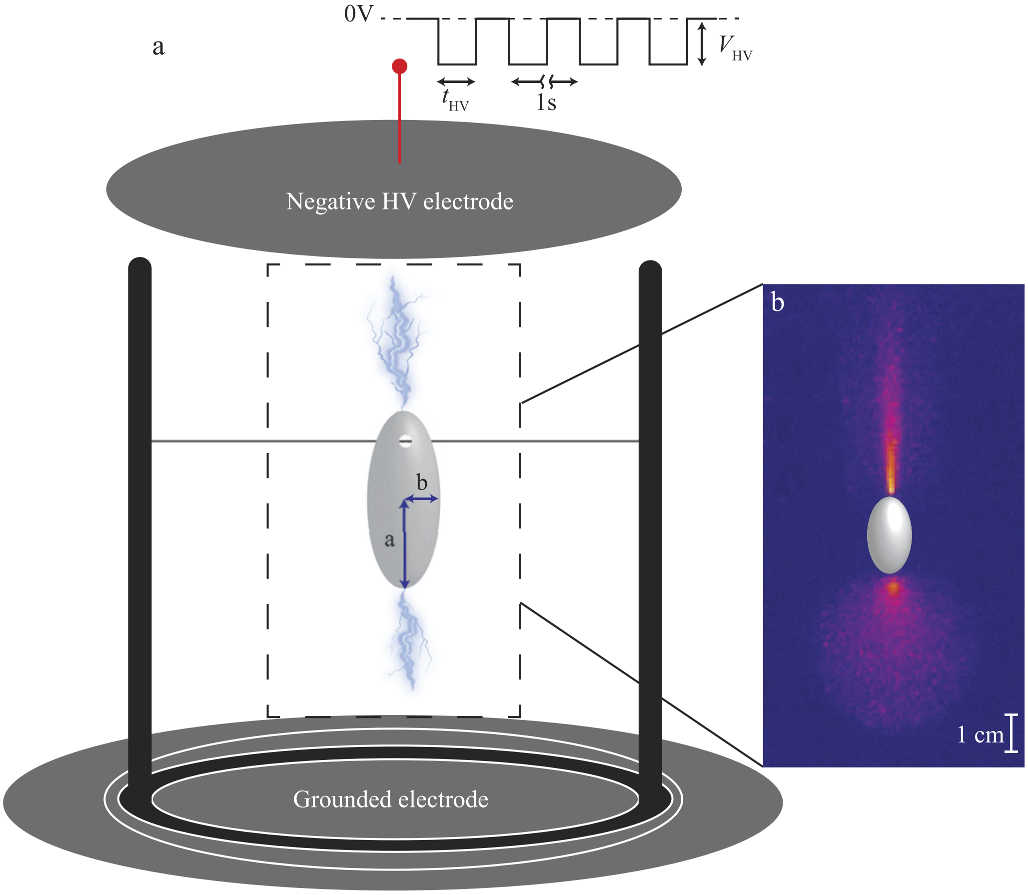

Figure 2. (a) schematic of the setup where an ellipsoid particle with semi-major axis a and semi-minor axis b is suspended by a thin fishing line between a negative high-voltage and grounded electrode. (b) ICCD image of streamer development from a dielectric particle ($a = 1$ cm and $b/a = 0.44$).

Table 1. List of metal and dielectric particles with different shapes and *AR*.

Length (cm)	Shape *R*/*L*	*AR* *b*/*a*	Material
8	0.1	0.44	TiO_2 and brass
	0.05	0.1	TiO_2 and brass
	0.01	0.044	Brass
4	0.1	0.44	TiO_2 and brass
	0.05	0.1	TiO_2 and brass
	0.01	0.044	Brass
2	0.1	0.44	TiO_2 and brass
	0.05	0.1	Brass
	0.01	0.044	NA
1	0.1	0.44	TiO_2 and brass
	0.05	0.1	Brass
	0.01	0.044	NA

positions in the two images by this delay time. Note that at the applied voltages, we observed low jitter (<5 ns) during streamer inception, which makes them reproducible. Before taking the images at each exposure time, we checked the ICCD images to ensure the reproducibility of the streamers.

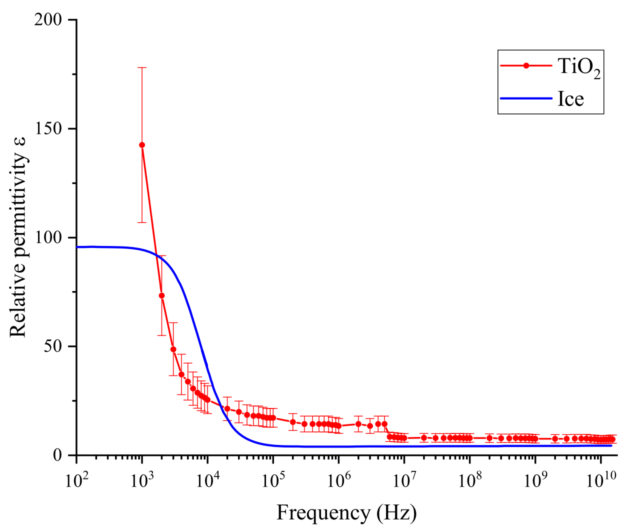

Figure 3. Measured relative permittivity of TiO_2 and ice. The data for ice was taken from [19].

Finally, the error bars show standard deviation of three independent experiments.

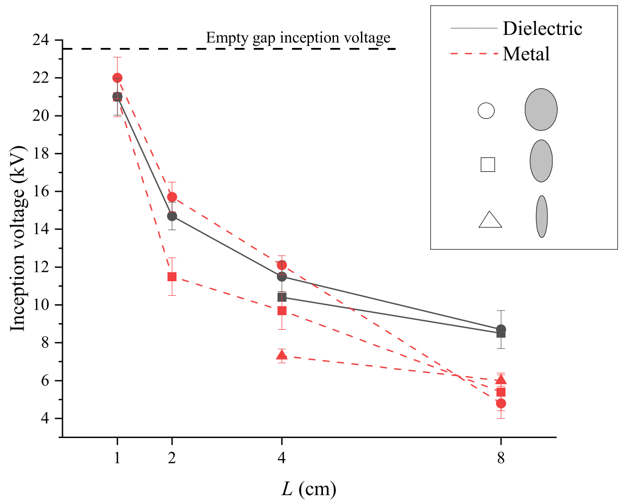

Figure 4. Inception voltage with the metal (red) and dielectric (black) particles for different L and AR at 50 mbar in air. ○, □ and △ represent data for the particles with $AR = 0.44$, 0.1 and 0.044, respectively. The dashed line shows the breakdown voltage without a particle in the gap. The error bars show standard deviation of three independent experiments.

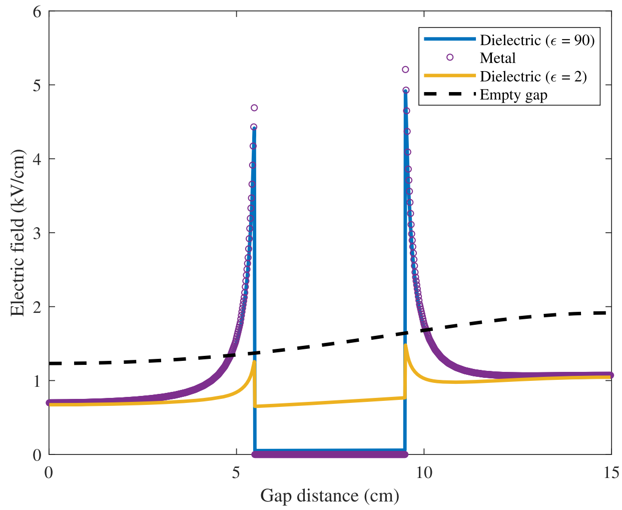

Figure 5. Electric field on the center axis of the gap as a function of gap distance to the grounded electrode for dielectric particles with a permittivity of 90 (blue), 2 (yellow) and metal particles (circle) ($L =$ 4 cm, $AR = 0.044$) and the gap without particles (dashed black). The high-voltage electrode (breakdown voltage of empty gap = 23 kV (dashed line) and others 12.5 kV) was placed at 15 cm, the grounded electrode was placed at 0 cm, and the particle was placed in the middle of the gap.

3. Results and discussion

3.1. Streamer inception from particles

We measured the streamer inception voltage from different metal and dielectric particles under a negative HV pulse with a pulse width of 10 μs. The inception voltage was the minimum voltage for which we observed a peak in the PMT signal. To support our observation, we made an ICCD-image with a camera gate of 10 μs to observe streamers at the inception voltage.

Figure 4 shows the streamer inception voltage from the metal and dielectric particles with different aspect ratios. The measured breakdown voltage for the empty gap is shown as a dashed line. It can be seen that the longer particles with the same aspect ratio had a lower inception voltage. The inception voltage for 8 cm dielectric particles decreased to less than half of the breakdown voltage. At the same length, the sharper particles generally had a lower inception voltage. For 4 cm metal particles, the inception voltage for particles with an aspect ratio of 0.044 was approximately half the inception voltage of the particles with an aspect ratio of 0.44. This was also observed for dielectric particles but less pronounced than for metal particles (the inception voltages of the dielectric particles with aspect ratios of 0.44 and 0.1 were 11.8 and 10.9 kV). Considering the particle materials, the difference between the inception voltages of metal and dielectric particles was not significant. For the 8 cm particles we observed that the inception voltage for metal particles is significantly lower than that of dielectric particles (6 ± 2 kV compared to 9 ± 1 kV). A possible reason may be surface charge density. A large dielectric particle with a larger surface area can carry more charge to influence the streamer initiation. We also observed a similar trend for 25 and 100 mbar pressures (data not shown). According to a previous simulation study [21] for larger charged particles, size and shape are the determining factors for the critical inception field value and not the surface charges, while for the smaller ones the surface charge accumulation is more important. Moreover, higher surface charge density results in a lower critical inception field. They considered a lower Meek number for discharge initiation criteria when they studied charged hydrometeors. According to their results for column hydrometeors with 0.8 mm tip size (similar to the smallest particle size in our experiments) that is charged by 200 pC the electrified strength is around 10^6 V m^{-1} compared to 0.5×10^6 V m^{-1} for a non-charged hydrometeor.

3.1.1. Electric field calculation. Using the electrostatic module in COSMOL multiphysics [22], we were able to calculate the electric field in the presence of dielectric and metal particles. For this purpose, a particle ($L = 4$ cm and $AR = 0.044$) was virtually suspended between two electrodes as described in section 2.1. For the dielectric particles, we used isotropic relative permittivity values of 90 and 2. For metal particles, we used a floating potential with no charge on it. In both cases, the top electrode was connected to 12.5 kV (the inception voltage according to figure 4). Additionally, to measure the empty gap inception voltage (at 50 mbar) between two electrodes, the particle was removed, and the top electrode voltage was set to 23.5 kV, as shown in figure 4. The results are shown in figure 5. The electric field increased near the particle tips to approximately 5 times the empty gap inception voltage. It is important to note that while the field enhancement is greater than the breakdown electric field, electrons need enough space to initiate an avalanche. Hence, streamers need to be initiated at an electric field higher than the breakdown field. Figure 5 shows the similarity between the electric field profile of the TiO_2 and metal particles. Obviously, a particle with a lower

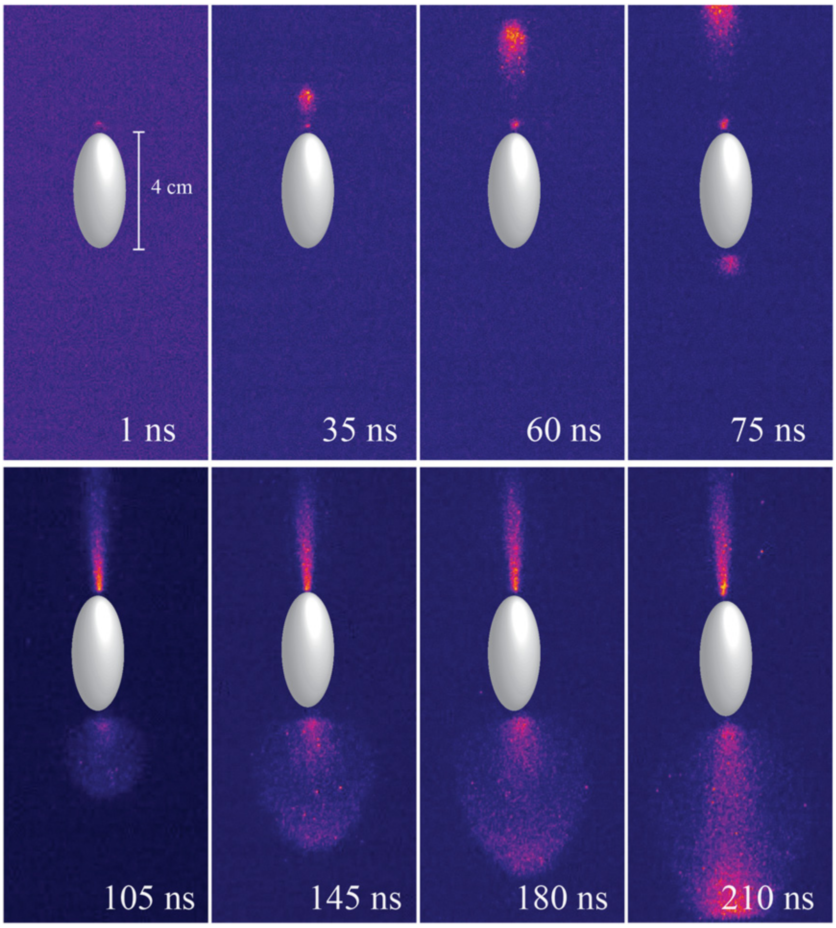

Figure 6. Phase resolved images of bipolar discharge development from a dielectric particle with $L = 4$ cm and $AR = 0.44$ in 50 mbar air with $V_{HV} = 15$ kV and $t_{HV} = 1$ μs in a gap of 15 cm. The camera gate time is 5 ns and the exposure start time with respect to the high voltage pulse is indicated in each image. Each image was taken from a different discharge event under the same conditions.

permittivity (e.g., $\epsilon = 2$) results in less field enhancement, and we expect to require a higher applied electric field to initiate a discharge. From the electric field profile, we can conclude that because of the similar electric field strength between TiO_2 and metal particles, their inception voltages should be close to each other. This is in line with our measurement in figure 4. Note that the asymmetry of the electric field between the top and bottom of the particle is due to the different sizes of the high-voltage and grounded electrodes. We have tried to compensate this effect by moving the particle closer to the top or bottom electrodes. However, it was not enough to have an equal electric field on the top and bottom of the particle. Furthermore, we did not include surface charge accumulation due to the repetitive pulse discharges on the dielectric particles in our calculations. This might have some effects on the inception voltage. We observed roughly similar profiles for particles with a length of 8 cm (data not shown). The results are in line with the previous modeling work of Dubinova *et al* [14] in which, at the same $AR = 0.01$, if the length of the hydrometeor increased by a factor of four, the inception voltage was halved (note that we perform the experiments in a finite gap).

3.2. Streamer development from particles

In this section, we study streamer development from the metal and dielectric particles. Figure 6 shows the streamer propagation from a dielectric particle with $L = 4$ cm and $AR = 0.44$ under a -15 kV, 1 μs HV pulse at 50 mbar. Since the top electrode was connected to a negative power supply, a positive streamer initiated from the top of the particle and propagated to the cathode. A positive streamer initiates first due to the lower initiation voltage of positive streamers [23–25]. After a propagation time of the positive streamers of approximately 75 ns, a discharge initiates on the bottom of the particle. Since negative charges accumulate on the bottom of the particle, a negative discharge begins to propagate toward the grounded electrode. An explanation for the negative streamer initiation is that the accumulated charges on the bottom of the particle are enough to produce the required electric field for its initiation. Negative streamers need higher inception fields than positive streamers. Therefore, the positive streamer must propagate some distance to increase the field at the bottom. A similar bipolar discharge from spherical hydrometers was investigated by [16], who showed that positive streamers precede negative streamers due to their lower inception fields. Furthermore, Luque *et al* [23] showed that for a double-headed streamer

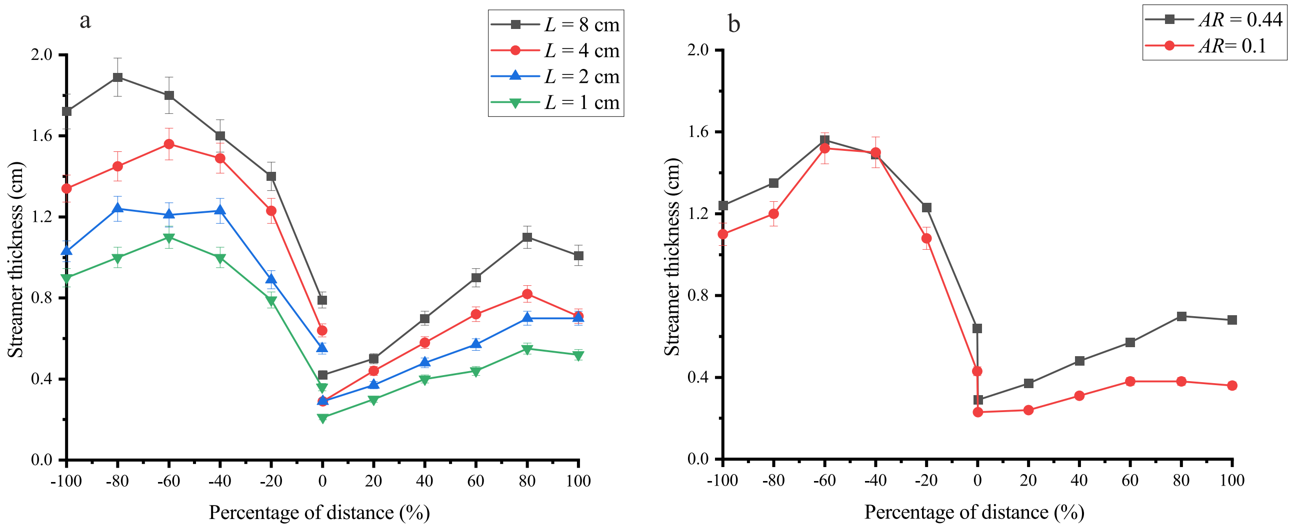

Figure 7. Streamer thickness measured from ICCD images from different stages of the streamer development from dielectric particles at 50 mbar in air when 15 kV is applied to the electrode (a) at a fixed $AR = 0.44$ and various values of L and (b) at a fixed $L = 4$ cm and different values of AR. The top electrode is placed at 100% and the bottom electrode at -100% while the top and bottom of the particle are located at 0%. The error bars show standard deviation of three independent experiments.

discharge, the negative discharge is wider than the positive discharge since negative streamers propagate in the direction of the electron drift. Moreover, they observed that positive streamers are faster than negative due to the higher field enhancement in the narrower positive streamers. In the next sections, we investigate the streamer thickness and velocity under different conditions. Similar results were obtained by [26].

3.2.1. Streamer thickness. Figure 7(a) shows the thickness of the positive and negative streamers as a function of distance percentage for dielectric particles with $AR = 0.44$. Here, it shows that positive and negative streamers become thicker during propagation. For $L = 4$ cm, the thickness increased to 0.5 cm at 80% of the gap. As the streamers approach the electrodes, we observe that the streamers became thinner. A possible reason for this is the higher electric field when streamers approach the electrodes. In this situation, the proximity effect occurs in which a counter-streamer can initiated from the electrode that can totally change the streamer behavior. Briels *et al* [27], measured streamer diameters created in a pin-to-plate setup at a reduced field ($V/(p \cdot d)$) of about 25 kV cm^{-1} bar^{-1} and found a minimal diameter of about 3 mm. This is close to our observations for the streamers that are initiated from the 1 cm length dielectric particle (which has a minimal effect in the shape of the electric field and has the sharpest tip). However, note that the basic setup configuration of that work is different from our research which might influence the electric field distribution in the gap.

When comparing particles with different lengths, we observe that streamers from longer particles are thicker. Positive streamers from the particle with a length of 8 cm are 1.8 times thicker than those from the 1 cm long particle at 40% of the gap. This ratio is the same for negative streamers although negative streamers are wider than positive streamers, as discussed above. This is mainly due to the higher field enhancement in the longer particles.

For a fixed L and varying AR for dielectric particles, figure 7(b) shows thicker positive streamers from thicker particles. For particles with $AR = 0.44$, the streamer thickness is 0.5 cm at 40% of the gap compared 3.7 mm for the particles with $AR = 0.1$. For negative streamers, the thicknesses are much closer, within the error margins.

3.2.2. Streamer velocity. We have plotted the measured the streamer propagation velocity in figure 8. We observe that longer metal and dielectric particles have higher propagation velocities. The streamer velocity for 8 cm long particles was almost twice that of particles with a length of 1 cm. In figure 7, we see that longer particles with the same shape had thicker and faster streamers. Moreover, streamer propagation from dielectric particles was faster than that from metal particles. For the 4 cm long particles, the velocity of streamers initiated by the dielectric particles was, on average, 1.2 times higher than that of streamers initiated from the metal particles. Figure 5 shows that the electric field enhancement near a TiO_2 particle was slightly less than near a metal particle. However, the average velocity of positive streamers from dielectric particles was higher than of those initiated from metal particles. A possible explanation is that we did not take the surface charge on the dielectric particles into account which might change the electric field distribution near the dielectric particle.

When comparing propagation velocities for different aspect ratios while keeping $L = 4$ cm fixed in figure 8(b), we see that positive streamers initiated by particles with a blunt tip are faster. The mean positive streamer velocity for a dielectric particle with $AR = 0.44$ was 7.5×10^5 m s^{-1}, while for a dielectric particle with $AR = 0.044$, this value was observed to be 5.1×10^5 m s^{-1}. Similar to our previous explanation, we observed that the streamer velocity from dielectric particles was higher than from metal particles.

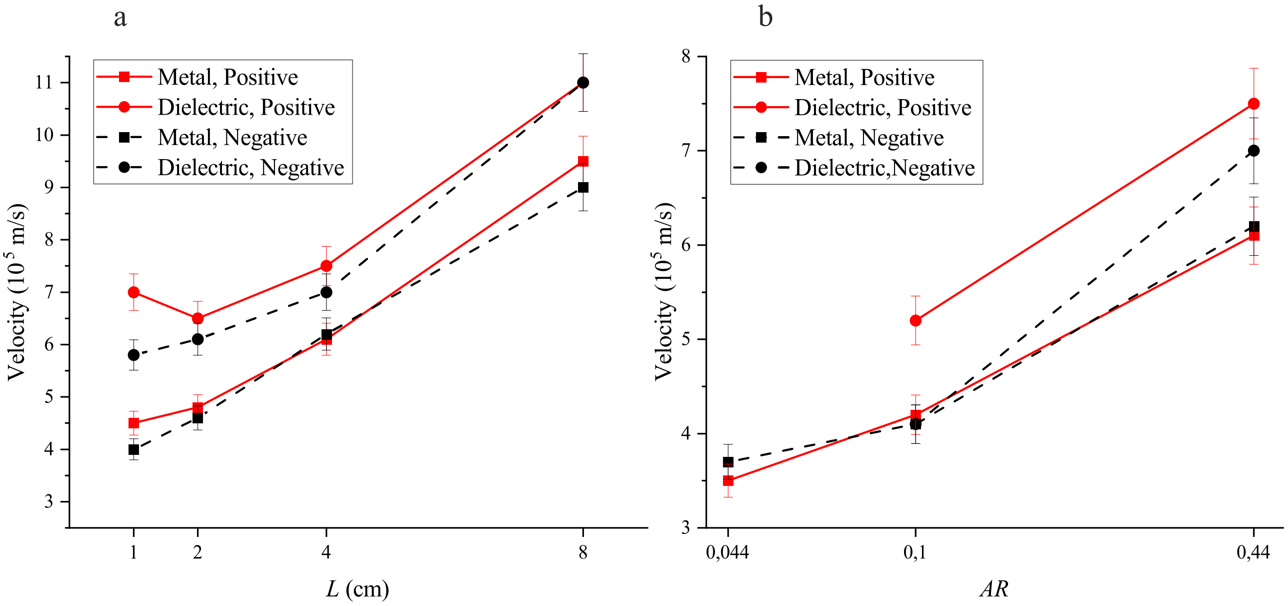

Figure 8. Velocity of streamers initiated by particles under a voltage of 15 kV at 50 mbar in air (a) at a fixed $AR = 0.44$ and various L, (b) at a fixed $L = 4$ cm and different AR. The error bars show standard deviation of three independent experiments.

Finally, we compare positive and negative streamers, and observe that positive streamers are slightly faster than negative streamers for the same conditions. This seems to be surprising at the first glance because for negative streamers the space-charge front propagates with the electron drift. However, as Luque *et al* [23] suggested and we observe in figure 7, a thinner positive streamers head leads to more field enhancement and consequently faster propagation while outward drift motion of electrons in negative streamers leads to a loss of focus of streamer head and subsequently decrease in field enhancement.

4. Summary and conclusions

In this work, we showed that streamers can be initiated from centimeter-size ellipsoidal particles at background fields significantly lower than the classical breakdown fields. In our experiments, we used dielectric particles with a similar profile to ice and compared them with metal particles. We observed that longer and sharper particles resulted in streamer inception as low as $0.4E_k$ (from an 8 cm, $AR = 0.44$ dielectric particle). This is in line with previous experimental results with ice crystals at low temperatures [11]. This shows that to initiate a discharge with field enhancement near a sharp tip, the minimum ionization area close to the tip must provide enough space for the electron avalanche process. This was also predicted by [14], who observed an optimal AR for inception, while a longer and sharper hydrometeor resulted in greater field enhancement near the tip but too little space to start an avalanche. Moreover, a recent simulation study by Hu *et al* [21] shows that the initiation electric field decreases for larger hydrometeors. They showed that with a large enough column-shaped hydrometeor, the critical electric field for streamer initiation can be as low as $0.3E_k$. Our particle sizes are initially based on a previous simulation study by Dubinova *et al* [14]. These particle sizes are on the extreme large side of observed hydrometeor size distributions in thunderclouds, as observations have shown that such hydrometeors only have a density of about 0.1 m^{-3} [28]. Note that in thunderclouds, there might be a system of multiple hydrometeors that can act as a large hydrometeor via inter-discharge connections between them. From the dielectric profile measurements and the results obtained during inception, we can conclude that metal particles are very similar to TiO_2 dielectric particles and ice. This shows that in future studies, metal particle models can be used to predict the streamer inception behavior.

A bipolar duo of a positive and a negative streamer initiates from both dielectric and metal particles. First, the positive streamer starts from the positive tip of the particle since positive streamers require a lower electric field to be initiated than negative streamers. After ≈75 ns, when the negative charge accumulation on the particle is sufficient, a negative streamer starts to propagate from the other tip of the particle. This phenomenon was also studied in a thundercloud [29, 30], where a long series of random and independent bipolar radio pulses were observed, which may originate from the synchronization of multiple hydrometeor discharges stimulated by low-energy electrons generated by the runaway breakdown process.

Negative streamers are thicker than positive streamers, due to outward drift of the electrons, the streamer head becomes wider which results in less field enhancement. This likely explains our observation that negative streamers are slower than positive streamers. Streamers initiated from longer and thicker particles are faster and thicker. Moreover, streamers from dielectric particles are slightly faster than those from metal particles. This last observation is contrary to our expectation since field enhancement near a metal particle is higher than near a dielectric particle. A possible reason for this finding is charge accumulation on the surface of the dielectric due to the leftover charges of the repetitive discharges, which was not included in our field calculations.

We performed our experiments at room temperature; however, it should be noted that in a thundercloud environment, most lightning may be initiated at altitudes of 4–9 km, where the temperature can be below freezing to −30 °C [31]. While [32] reported a significant decrease in the corona current below −18 °C, Petersen *et al.* [33] showed that positive streamers can initiate from ice crystals at temperatures as low as −38 °C. Moreover, Petersen *et al* [11] showed that at for constant pressure and ice crystal length, lower temperatures will lead to increased onset fields.

The next parameter to be considered is the source of the very first electron. In thunderclouds, cosmic rays can produce the free electrons that are required for the inception, and Dubinova *et al* [14] predicted that to initiate a discharge, 100 free electrons cm^3 are required. Another possible free electron source is electron detachment from metastable oxygen and nitrogen, as suggested by Lowke [34]. In our experiment, we exert the experiments under repetitive pulsed conditions. Previously, we have shown that in repetitive discharges, due to a memory effect, an inhomogeneous distribution of negative ions can be formed and remain for a long time in the gap, which can influence the discharge inception in the preceding pulses [35]. This can induce different effects on the inception voltage and differentiates it from the real situation in thunderclouds.

In summary, we showed that streamers can be initiated from dielectric and metal particles at background electric fields far below the classical breakdown electric field. A bidirectional positive and negative streamer was observed initiating from the tips of the particles.

Acknowledgments

This project has received funding from the European Union's Horizon 2020 research and innovation program under the Marie Sklodowska-Curie Grant Agreement 722337.

Data availability statement

The data generated and/or analysed during the current study are not publicly available for legal/ethical reasons but are available from the corresponding author on reasonable request.

ORCID iDs

S Mirpour https://orcid.org/0000-0002-4012-1136
S Nijdam https://orcid.org/0000-0002-1310-6942

References

[1] Petersen D, Bailey M, Beasley W H and Hallett J 2008 *J. Geophys. Res. Atmos.* **113** D17205
[2] Mazur V 2016 *Principles of Lightning Physics* (Bristol: IOP Publishing)
[3] Rakov V A and Uman M A 2003 *Lightning: Physics and Effects* (Cambridge: Cambridge University Press)
[4] Dwyer J R and Uman M A 2014 *Phys. Rep.* **534** 147–241
[5] Marshall T C, McCarthy M P and Rust W D 1995 *J. Geophys. Res.* **100** 7097–103
[6] Griffiths R and Phelps C 1976 *J. Geophys. Res.* **81** 3671–6
[7] Kostinskiy A Y, Marshall T C and Stolzenburg M 2020 *J. Geophys. Res. Atmos.* **125** e2020JD033191
[8] Meek J M 1940 *Phys. Rev.* **57** 722–8
[9] Montijn C and Ebert U 2006 *J. Phys. D: Appl. Phys.* **39** 2979
[10] Laan M and Paris P 1994 *J. Phys. D: Appl. Phys.* **27** 970
[11] Petersen D, Bailey M, Hallett J and Beasley W 2015 *Q. J. R. Meteorol. Soc.* **141** 1283–93
[12] Mazur V, Taylor C D and Petersen D A 2015 *J. Geophys. Res. Atmos.* **120** 10–879
[13] Sadighi S, Liu N, Dwyer J R and Rassoul H K 2015 *J. Geophys. Res. Atmos.* **120** 3660–78
[14] Dubinova A, Rutjes C, Ebert U, Buitink S, Scholten O and Trinh G T N 2015 *Phys. Rev. Lett.* **115** 015002
[15] Dubinova A A 2016 Modeling of streamer discharges near dielectrics *PhD Thesis* Department of Applied Physics, Technische Universiteit Eindhoven
[16] Gao X, Liu N, Shi F and Rassoul H K 2020 *J. Electrost.* **106** 103457
[17] Wu J, Gao X, Ma Y and Liu N 2019 *Plasma Res. Express* **1** 035009
[18] Peeters S A, Mirpour S, Köhn C and Nijdam S 2022 *J. Geophys. Res. Atmos.* **127** e2021JD035505
[19] Mavrovic A, Roy A, Royer A, Filali B, Boone F, Pappas C and Sonnentag O 2018 *Geosci. Instrum. Method. Data Syst.* **7** 195–208
[20] Nijdam S, van de Wetering F M J H, Blanc R, van Veldhuizen E M and Ebert U 2010 *J. Phys. D: Appl. Phys.* **43** 145204
[21] Hu J, Ma Y, Gao X and Liu N 2021 *J. Geophys. Res. Atmos.* **126** e2021JD034936
[22] COMSOL Multiphysics® v. 5.4, http://comsol.com Stockholm, Sweden (COMSOL AB)
[23] Luque A, Ratushnaya V and Ebert U 2008 *J. Phys. D: Appl. Phys.* **41** 234005
[24] Briels T, Kos J, Winands G, van Veldhuizen E and Ebert U 2008 *J. Phys. D: Appl. Phys.* **41** 234004
[25] Nijdam S, Teunissen J and Ebert U 2020 *Plasma Sources Sci. Technol.* **29** 103001
[26] Sun A, Teunissen J and Ebert U 2014 *J. Phys. D: Appl. Phys.* **47** 445205
[27] Briels T M, Winands G, Nijdam S, van Veldhuizen E and Ebert U 2011 Exploring streamer variability in experiments *PhD Thesis* Department of Applied Physics, Technische Universiteit Eindhoven
[28] Lamb D and Verlinde J 2011 *Physics and Chemistry of Clouds* (Cambridge: Cambridge University Press)
[29] Gurevich A and Karashtin A 2013 *Phys. Rev. Lett.* **110** 185005
[30] Montanyà J, Van Der Velde O and Williams E R 2015 *Sci. Rep.* **5** 15180
[31] Proctor D E 1991 *J. Geophys. Res.* **96** 5099–112
[32] Griffith R F 1975 *J. Electrost.* **1** 3–13
[33] Petersen D, Bailey M, Hallett J and Beasley W H 2006 *Q. J. R. Meteorol. Soc.* **132** 263–73
[34] Lowke J 2015 *J. Geophys. Res. Atmos.* **120** 3183–90
[35] Mirpour S, Martinez A, Teunissen J, Ebert U and Nijdam S 2020 *Plasma Sources Sci. Technol.* **29** 115010